J|A|C|S ARTICLES

Published on Web 11/16/2010

Controlling the Structure of Proteins at Surfaces

Michael Geisler,[†] Senbo Xiao,[‡] Elias M. Puchner,[§,#] Frauke Gräter,[‡,||] and Thorsten Hugel*[,†]

IMETUM, Physics Department, CeNS and CIPSM, Technische Universität München, 85748 Garching, Germany, Key Laboratory for Computational Biology, MPG-CAS Partner Institute for Computational Biology, Chinese Academy of Sciences, 200031 Shanghai, China, Bioquant, Heidelberg University, 69120 Heidelberg, Germany, and Center for Nanoscience and Department of Physics, University of Munich, 80799 Munich, Germany

Received August 20, 2010; E-mail: thorsten.hugel@ph.tum.de

Abstract: With the help of single molecule force spectroscopy and molecular dynamics simulations, we determine the surface-induced structure of a single engineered spider silk protein. An amyloid like structure is induced in the vicinity of a surface with high surface energy and can be prohibited in the presence of a hydrophobic surface. The derived molecular energy landscapes highlight the role of single silk protein structure for the macroscopic toughness of spider silk.

Introduction

In many applications, proteins or polypeptides have to be immobilized at surfaces.[1,2] To keep their functionality, conformational changes in polypeptides or even denaturation of proteins induced by substrates have to be avoided. Evidence has accumulated that already soft surfaces like lipid membranes can cause polypeptides to lose their functionality by forming amyloid-like secondary structures[3,4] related to recognized clinical disorders, including type II diabetes, and Alzheimer disease.[5] Yet is it also possible to use this obstacle to our advantage by creating functionality through surface contact? Key to answer this question are molecular forces involved in the structure formation and how these forces are affected by thermodynamic parameters. Here, we use force spectroscopy to monitor structural changes with one and the same single polypeptide. We show that structure formation within a single protein, a genetically engineered variant of spiders dragline silk, eADF4, which consists of 16 identical repeats,[6] is induced in the vicinity of surfaces with high surface energy and can be prohibited in the presence of hydrophobic surfaces. In addition, we investigated how salts and temperature modulate surface-induced folding. The experimentally determined molecular structure agrees well with force probe molecular dynamics (FPMD) simulations. This surface-induced structure bears striking similarities to the conformation of amyloidogenic peptides in their fibrilar assemblies and gives insight into the molecular origin of the enormous energy absorption and strength-bearing properties of silk threads.

Results and Discussion

For the following experiments, a single eADF4 molecule has been covalently attached with its N-terminus via a long flexible linker of poly(ethylene glycol) (PEG) to an atomic force microscopy (AFM) cantilever tip (Figure 1a, experimental details are given in the Supporting Information). Covalent bonding provided the necessary long-term stability to allow measurements for hours with one and the same protein on different substrate materials in solution. The tip with the protein was brought in contact with the surface for 1 s to adsorb and possibly to form its fold before being retracted at a velocity of 1 μm/s.

Up to 48 °C, we obtain velocity-independent force plateaus (Figure 1b) with a length equal to the contour length of the protein. Accordingly, the desorption of eADF4 from its N-terminus to its C-terminus occurs in equilibrium, and stable structural features are absent.[7] As can be seen from Figure 1b, the traces above 48 °C on stainless steel 316 L, which is one of the most common alloys in medicine, are considerably different. Here, a regular pattern of peaks with amplitudes ranging from 70 to 200 pN appears on top of the desorption plateaus. Such regular peaks are the characteristic fingerprint for unfolding secondary structures.[8,9] This was the only structure observed in many traces with different cantilever tips and therefore represents the protein conformation. It is highly unlikely that the passivated tip alters or destroys the structure each time and in each experiment in exactly the same way. We still probe the

[†] Technische Universität München.
[‡] Chinese Academy of Sciences and Heidelberg University.
[§] University of Munich.
[||] Present address: HITS gGmbH, Schlosswolfsbrunnenweg 35, 69118 Heidelberg, Germany.
[#] Present address: Department of Cellular and Molecular Pharmacology, UCSF, CA 94158.

(1) Goel, A.; Vogel, V. *Nat. Nanotechnol.* **2008**, *3*, 465–75.
(2) Sarikaya, M.; Tamerler, C.; Jen, A. K.; Schulten, K.; Baneyx, F. *Nat. Mater.* **2003**, *2*, 577–85.
(3) Capriotti, L. A.; Beebe, T. P., Jr.; Schneider, J. P. *J. Am. Chem. Soc.* **2007**, *129*, 5281–7.
(4) Domanov, Y. A.; Kinnunen, P. K. *J. Mol. Biol.* **2008**, *376*, 42–54.
(5) Dobson, C. M. *Nature* **2003**, *426*, 884–890.
(6) Rammensee, S.; Slotta, U.; Scheibel, T.; Bausch, A. R. *Proc. Natl. Acad. Sci. U.S.A.* **2008**, *105*, 6590–6595.
(7) Horinek, D.; Serr, A.; Geisler, M.; Pirzer, T.; Slotta, U.; Lud, S. Q.; Garrido, J. A.; Scheibel, T.; Hugel, T.; Netz, R. R. *Proc. Natl. Acad. Sci. U.S.A.* **2008**, *105*, 2842–2847.
(8) Cao, Y.; Kuske, R.; Li, H. B. *Biophys. J.* **2008**, *95*, 782–788.
(9) Rief, M.; Gautel, M.; Oesterhelt, F.; Fernandez, J. M.; Gaub, H. E. *Science* **1997**, *276*, 1109–1112.

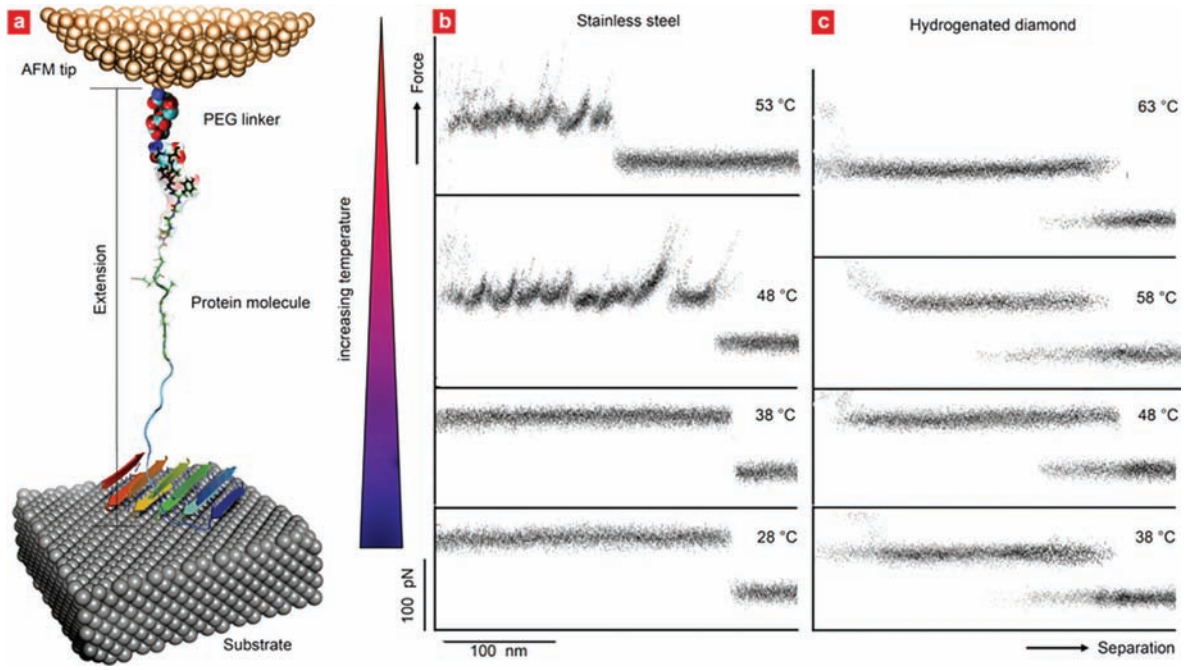

Figure 1. Monitoring surface-induced protein folding in eADF4. (a) Sketch of the single molecule desorption experiment of eADF4 attached to the AFM tip via a PEG linker (not to scale). Here, the molecule exhibits β-sheet structure on the steel surface. (b) Force−extension traces of a single eADF4 molecule in water at varying temperatures desorbed from stainless steel and (c) from hydrogenated diamond. Each graph shows the superposition of 20 consecutive force−separation curves.

full contour length of eADF4 at 48 °C, and hence the unfolding of all structural elements. The observation of a desorption plateau underlying the peaks is a fingerprint for a very high mobility in the surface plane and excludes the presence of distinct adhesion sites in this plane. In other words, the peptide is removed (perpendicular to the surface plane) in steps, which are defined by the stability of its secondary structure, while it is highly mobile in the surface plane.

All data in Figure 1b were recorded with one and the same eADF4 molecule as indicated by the single step drop of the force plateau to the zero line.[10] The only parameter that was varied was the solution temperature. We identified the temperature around 48 °C as the transition temperature for structure formation on hydrophilic stainless steel. A second set of experiments in Figure 1c substantiates that the structure is not formed in solution but is surface-induced, because the same experiments on hydrophobic, hydrogenated diamond show no conformational transition (even up to 63 °C). Not only temperature, but also a higher ionic strength of phosphate of about 100 mM can facilitate the transition in line with previous bulk experiments,[11] but again only on the hydrophilic metal substrate (Supporting Information Figure S2.1). The reason probably is the polar character and thus the high interfacial energy of steel of 38 mJ/m^2 as compared to 18 mJ/m^2 for the diamond substrate (determined by contact angle measurements).

What are the characteristic features underlying the surface-induced structure of eADF4? Following previously described methods,[12] we transformed the 20 force−extension traces from Figure 2a into contour length space and obtained histograms

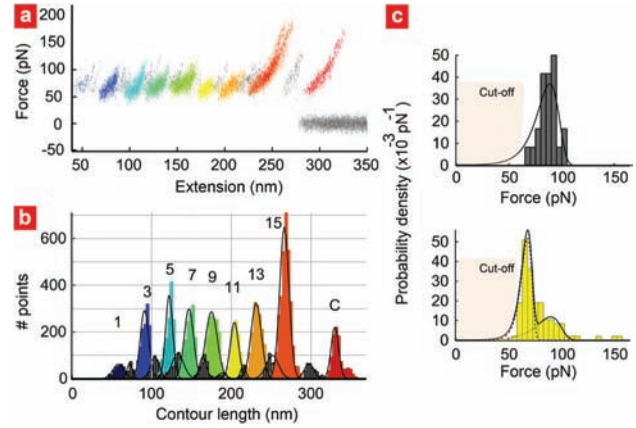

Figure 2. Forced unfolding of the eADF4 structure. (a) Superposition of 20 force−extension traces of eADF4 with odd peaks being marked in color. The traces were recorded in salt solution on steel (316 L) at room temperature. (b) Averaged barrier position histogram obtained by transformation of each of the 15 unfolding peaks with a persistence length of 5.1 Å into contour length space and averaging the 20 resulting barrier position histograms for each peak. (c) Unfolding force distributions and normalized unfolding probability density for two sequential unfolding barriers (same color coding). The shaded area in the lower force regime illustrates the resolution limit of the instrumentation (cut-off). The best fit to the data (solid black) reveals two discrete barrier binding potentials: a low force unbinding around 75 pN (dashed) and high force unbinding around 90 pN (dotted).

that directly reflect particular locations along the polymer contour that constitute an energy barrier for unfolding (Figure 2b). The histogram shows 16 equidistant unfolding barriers corresponding to the 16 repeats of eADF4 plus one terminal barrier originating from the detachment of the C-terminus from the surface. For a detailed analysis of the force distributions, well-defined loading rate conditions (constant spacer lengths)

(10) Geisler, M.; Balzer, N. B.; Hugel, T. *Small* **2009**, *5*, 2864–2869.
(11) Lammel, A.; Schwab, M.; Slotta, U.; Winter, G.; Scheibel, T. *ChemSusChem* **2008**, *1*, 413–416.
(12) Puchner, E. M.; Franzen, G.; Gautel, M.; Gaub, H. E. *Biophys. J.* **2008**, *95*, 426–434.

Table 1. Potential Width (Δx_{pp} and Δx_{ap}) and Unfolding Rate Constants (k_{pp}^{off} and k_{ap}^{off}) at Zero Force (Water, 48 °C) for Parallel and Anti-parallel Arrangements, Respectively[a]

	event no.												
	1	2	3	4	5	6	7	8	9	11	13	15	17
Δx_{pp} (Å)	8.5		8.6		8.7		9.0		8.3	9.9	9.3	3.0	4.6
k_{pp}^{off} (10^{-4} s^{-1})	1.3		1.5		1.4		1.4		1.5	1.6	1.5	1×10^3	2×10^2
Δx_{ap} (Å)	4.7	4.0	5.1	4.8	4.9	4.9	4.5	4.9	4.5	4.6	4.8	1.4	1.7
k_{ap}^{off} (10^{-2} s^{-1})	3.0	3.0	3.5	3.6	3.0	3.6	3.0	3.9	3.2	3.5	3.0	55	55

[a] The unbinding events are numbered sequentially starting at the N-terminus.

are essential.[13] Therefore, all 16 rupture peaks have to be analyzed separately. Figure 2c displays two consecutive force histograms out of the 16 together with their probability functions fitted to the data based on the assumption of a one-barrier binding potential[13−15] (for details, see Supporting Information S3). These histograms differ from odd to even unfolding events. The former have to be fitted with two separate potentials, while the even barrier numbers can be fitted with one. The potential widths derived from these probability functions are all summarized in Table 1. We find a short potential width of 4.7 Å for high force unfolding and a longer width of 8.9 Å for all low range forces. Only the last two values are different due to the influence of the C-terminus interacting with the substrate. Our study of the conformational transition caused by increased salt concentration on steel yields similar values and suggests an equal folding mechanism (see Supporting Information S2). The high mobility in the plane of the surface and the two different barriers cannot be explained by the strong interaction of a single amino acid in a repeat unit of eADF4. The slight broadening of the rupture force peaks and the analogy of the transition barrier distances to diffraction patterns of amyloidogenic structures make the $(Ala)_8$ repeats very likely candidates for the observed structure.

To relate these data to three-dimensional surface-adhered structures of eADF4, we therefore modeled structures formed by the amyloidogenic repeat units of eADF4, that is, $(Ala)_8$, to assess their mechanical response using FPMD simulations (see Supporting Information S4). Force fields for steel−protein interactions are not available yet,[16] but previous studies of amino acids on noble metals have found polar interactions to prevail.[17,18] We here assume steel to mainly serve as a template, inducing order in the poly(Ala) segments similar to the role of shear flow in silk fibrillogenesis. The backbone amide groups in $(Ala)_8$ are polar and therefore likely candidates to orient toward the hydrophilic metal surface (see Supporting Information S4). We assembled a two-layer β-sheet, consisting of $(Ala)_8$ β-strand motifs connected by interstrand hydrogen bonding, that are stacked against each other via side-chain interactions parallel to the surface plane (Figure 3a). Coil domains of eADF4 were omitted in the simulations (see Supporting Information S5). The various relative orientations in a double layer can be grouped into antiparallel, parallel, and mixed arrangements (Figure 3a).

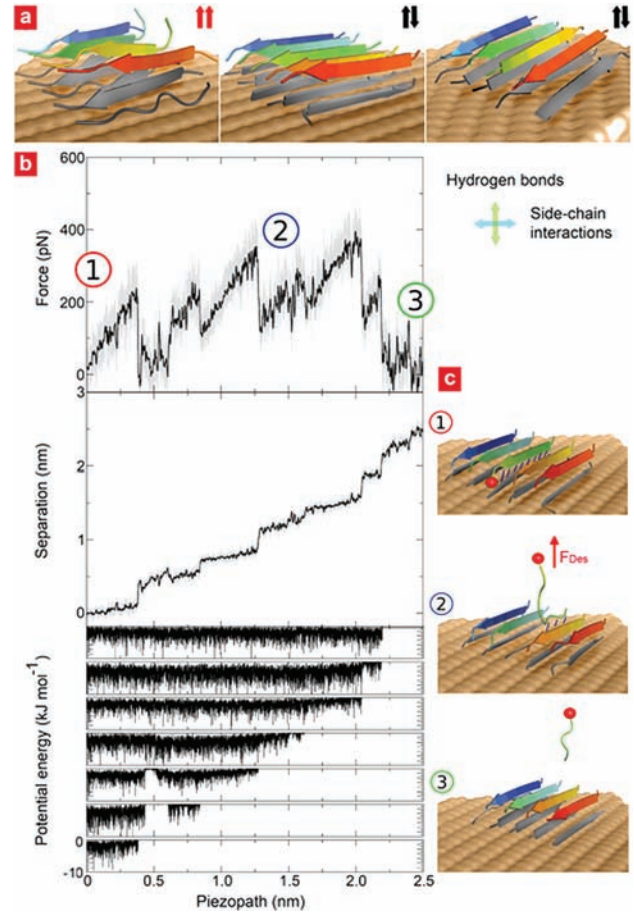

Figure 3. Surface-induced structures probed by force-probe MD simulations. (a) Modeled two-layer $(Ala)_8$ arrangements: all parallel on the left, mixed in the middle, and all antiparallel on the right. Red and black arrows make the connection to the energy landscapes in Figure 3D. Directions of hydrogen bonds and side-chains are indicated. (b) Representative FPMD simulation of rupturing one strand from the upper layer of the antiparallel structure. Shown are the force profile (top), the displacement of the pulled group from which Δx is estimated (middle), and potential energies of hydrogen bonds between the pulled strand and its neighbors (bottom). (c) Simulation snapshots, with hydrogen bonds shown as blue sticks, are numbered to indicate the corresponding position on the force profile.

From FPMD simulations, we find independently from the detailed arrangement strands in the upper layer of the crystalline structure that detach with forces of 250−450 pN. These forces are due to the rupture of strong hydrogen bonds to the adjacent bottom strand (Figure 3b). The subsequent rupture of the bottom strand, not stabilized by interstrand hydrogen bonds anymore but only adsorbed to the surface, does not give rise to a force peak. This also implies that a one-layer arrangement would lead to a mere force plateau and thus cannot explain the experimental force pattern. We note that the experimental distances to the

(13) Friedsam, C.; Wehle, A. K.; Kuhner, F.; Gaub, H. E. *J. Phys.: Condens. Matter* **2003**, *15*, S1709–S1723.
(14) Carrion-Vazquez, M.; Marszalek, P. E.; Oberhauser, A. F.; Fernandez, J. M. *Proc. Natl. Acad. Sci. U.S.A.* **1999**, *96*, 11288–11292.
(15) Evans, E.; Ritchie, K. *Biophys. J.* **1997**, *72*, 1541–1555.
(16) Cohavi, O.; Corni, S.; De Rienzo, F.; Di Felice, R.; Gottschalk, K. E.; Hoefling, M.; Kokh, D.; Molinari, E.; Schreiber, G.; Vaskevich, A.; Wade, R. C. *J. Mol. Recognit.* **2010**, *23*, 259–62.
(17) Ghiringhelli, L. M.; Hess, B.; van der Vegt, N. F. A.; Delle Site, L. *J. Am. Chem. Soc.* **2008**, *130*, 13460–13464.
(18) Schravendijk, P.; Ghiringhelli, L. M.; Delle Site, L.; van der Vegt, N. F. A. *J. Phys. Chem. C* **2007**, *111*, 2631–2642.

transition state are wider than those from simulations by a factor of about 3, most probably due to temperature softening,[19] but the relative changes match very well. Strikingly, strands in antiparallel arrangements show higher forces and smaller transition distances than those in parallel arrangements (Supporting Information S6), as previously found for the structurally related silk crystalline units in bulk.[20] These differences qualitatively agree with the two discrete unfolding barriers for odd numbered peaks observed in our AFM experiments (Figure 2c and Table 1). One also has to consider strand−turn−strand motifs to be surface-assembled such that the pulling force acts onto the strand in the lower layer first, resulting in a concurrent detachment of the whole motif and therefore causing higher forces, as observed for the rare peaks with even numbers in Figure 2b and in corresponding FPMD simulations (Supporting Information S7). Finally, the plateau of constant force underlying the unfolding pattern stems from the desorption of the glycine-rich coiled segments between the poly(Ala) patches, which behave like a nonstructured flexible polymer with high in-plane mobility. When detaching a β-strand−coil−β-strand motif from within the two-layer β-sheet system as described above, we observe the structure to self-heal by sealing the introduced flaw on the nanosecond time scale of the simulations (Supporting Information S8).

Taken together, our structural model of a single eADF4 molecule derived from force spectroscopy matches the MD simulations. It also shows remarkable similarities with eADF4 assembled into nanofibrils and into microspheres[21] and with typical protein structures within amyloid aggregates.[22] Our combined experimental and theoretical data suggest parallel β-sheets to outnumber antiparallel counterparts in the surface-induced assembly. This is in contrast to the observed preference of antiparallel β-sheets of many amyloidogenic peptides,[22] but consistent with the parallel/antiparallel mixture in silk fibres determined by Asakura et al.[23]

In the following, we quantify the stability of the molecular structure and its origin. The parallel structure exhibits a very low mean transition rate of 1.5×10^{-4} s^{-1} and therefore high stability, which compares, for example, to that of the strong immunoglobulin fold of the muscle protein titin,[9] to ubiquitin,[24] or to the extracellular matrix protein tenascin.[25] In contrast, the mean transition rate of the antiparallel β-sheet formed by eADF4 (3.3×10^{-2} s^{-1}) is 2 orders of magnitude higher and is similar to those of calmodulin[26] and F-actin cross-linker filamin.[19] Assuming an Arrhenius prefactor of 10^7 s^{-1} (see Supporting Information S3), the transition energy can be calculated (Figure 4a). Remarkably, the parallel structure, which breaks first under load, is stronger and hence more stable at zero force and will therefore rapidly reform the moment the molecule relaxes.[27]

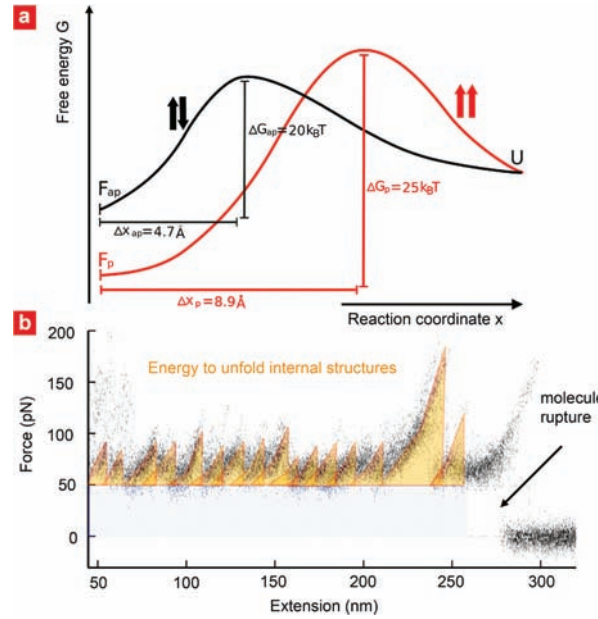

Figure 4. Strength-bearing properties and energy absorption of eADF4. (a) Schematic energy landscapes with potential widths (Δx) and energy barrier heights (ΔG) for unfolding parallel (red) and antiparallel (black) sheets from the folded (F) to the unfolded (U) state. (b) The area under the superposition of 20 typical force−extension traces of eADF4 is divided into the free energy contribution due to the equilibrium desorption (gray) at negligible energy dissipation (friction) and the energy that is needed to break individual elements of the secondary structure (orange) on steel 316 L at 48 °C.

The wider potential renders it more susceptible to force-induced destabilization.[28]

This raises the interesting question whether the final fiber properties are mirrored at the molecular level by a single protein. The toughness of a spider silk fiber from *Araneus* is 160 MJ m^{-3} [29] and corresponds to its energy to breakage. The number of molecular strands per fiber volume has been estimated to be of the order of 10^{26} strands per m^3.[30] If we now take the irreversible work on a single eADF4 polypeptide in our AFM experiment (Figure 4b), and consider the estimate that 40% of the silk fiber adopt β-sheet conformation,[29] we obtain an upper bound for the average toughness of 237 MJ m^{-3} (Supporting Information S9). The good agreement with experiments on silk fibers[29] underlines that structuring at the level of individual molecules quantitatively determines dissipation of mechanical energy at the macroscopic scale.

Conclusion

We have shown that single engineered silk proteins can form secondary structures in a solid substrate, salt, and temperature-dependent manner. On hydrogenated diamond no secondary structure was observed, while the stainless steel induced an amyloid like secondary structure. A control of such surface-induced structures should not only help to sustain the functionality of protein coated devices, but also to create new ones. Finally, our combined approach of single molecule force spectroscopy and MD simulations allowed us to determine the

(19) Schlierf, M.; Rief, M. *J. Mol. Biol.* **2005**, *354*, 497–503.
(20) Xiao, S. B.; Stacklies, W.; Cetinkaya, M.; Markert, B.; Grater, F. *Biophys. J.* **2009**, *96*, 3997–4005.
(21) Slotta, U. K.; Rammensee, S.; Gorb, S.; Scheibel, T. *Angew. Chem., Int. Ed.* **2008**, *47*, 4592–4594.
(22) Makin, O. S.; Serpell, L. C. *FEBS J.* **2005**, *272*, 5950–5961.
(23) Asakura, T.; Okonogi, M.; Nakazawa, Y.; Yamauchi, K. *J. Am. Chem. Soc.* **2006**, *128*, 6231–6238.
(24) Carrion-Vazquez, M.; Li, H. B.; Lu, H.; Marszalek, P. E.; Oberhauser, A. F.; Fernandez, J. M. *Nat. Struct. Biol.* **2003**, *10*, 738–743.
(25) Oberhauser, A. F.; Marszalek, P. E.; Erickson, H. P.; Fernandez, J. M. *Nature* **1998**, *393*, 181–185.
(26) Junker, J. P.; Ziegler, F.; Rief, M. *Science* **2009**, *323*, 633–637.
(27) Becker, N.; Oroudjev, E.; Mutz, S.; Cleveland, J. P.; Hansma, P. K.; Hayashi, C. Y.; Makarov, D. E.; Hansma, H. G. *Nat. Mater.* **2003**, *2*, 278–283.
(28) Hanke, F.; Kreuzer, H. J. *Phys. Rev. E* **2006**, *74*, 031909.
(29) Gosline, J. M.; Guerette, P. A.; Ortlepp, C. S.; Savage, K. N. *J. Exp. Biol.* **1999**, *202*, 3295–3303.
(30) Termonia, Y. *Macromolecules* **1994**, *27*, 7378–7381.

response of the surface-induced structure to an external force and provides an explanation for the toughness of spider silk threads.

Acknowledgment. We thank Ute Slotta and Thomas Scheibel for providing the eADF4 protein and Michael Schlierf for his help with the unfolding probability analysis. Helpful discussions with Hermann Gaub, Dominik Horinek, Paavo Kinnunen, Roland R. Netz, Matthias Rief, and Nico van der Vegt are gratefully acknowledged. We thank the DFG (Hu 997/7), NIM, and the ESF (Euromembrane Program) for financial support. M.G. was supported by the Elitenetzwerk Bayern in the framework of CompInt and by the Stiftung Industrieforschung. E.M.P. was supported by the DFG.

Supporting Information Available: Detailed description of the experimental methods, material, and simulation methods; salt-induced transitions; amorphous chain segments; and Figures S1−S8. This material is available free of charge via the Internet at http://pubs.acs.org.

JA107212Z